Characterizing the Effect of Freeman-Sheldon Syndrome Mutation T178I on Embryonic Myosin Function In Vitro

Molly Madden

Molecular, Cellular, and Developmental Biology
Departmental Honors Thesis

University of Colorado, Boulder
Defense Date: November 3rd 2020

Thesis Advisor: Dr. Leslie Leinwand (MCDB)

Honors Council Representative: Dr. Pamela Harvey (MCDB)

Third Member: Dr. Kristi Anseth (Chemical and Biological Engineering)

Abstract

Freeman-Sheldon Syndrome (FSS) is a rare skeletal muscle disease characterized by birth defects including a small mouth opening and malformation of the hands and feet. It is caused by point mutations in the embryonic myosin gene, which encodes a muscle motor protein, but the mechanisms by which a mutation disrupts fetal muscle development are not understood. To better understand FSS pathogenesis, the most clinically severe mutation (T178I) was studied at the molecular level to determine its impact on myosin motor function, and at the cellular level to determine the initial cellular response to potential changes in myosin behavior. The molecular effects of T178I on myosin's enzymatic activity and mechanical motor function were measured using *in vitro* ATPase and motility assays, respectively, to help elucidate the disease trigger. The data shows a trend of increased actin affinity for the T178I mutation compared to WT myosin. To study the compensatory response, we designed a gene-editing strategy to express T178I in mouse myoblast cells, which will be studied during muscle differentiation in culture.

Introduction

Freeman-Sheldon Syndrome (FSS) is a rare skeletal muscle disease characterized by birth defects such as a small mouth opening and malformation of the hands and feet. FSS is most prevalently caused by point mutations found in the ATP binding pocket of embryonic myosin, a muscle motor protein responsible for the contraction of skeletal muscle. Sarcomeric myosin, including embryonic myosin, are motor proteins that form the contractile filaments of muscle cells. Myosin organizes into a protein polymer called the thick filament. The thick filament interacts with the thin filament, an actin polymer network, forming the sarcomere which is the contractile unit within skeletal and cardiac muscle cells.

The FSS causing mutation is found in embryonic myosin which is the most abundant sarcomeric myosin expressed during development. Postnatally, however, embryonic myosin is heavily downregulated yet an FSS phenotype persists but does not worsen in adulthood. This phenotype is characterized by a whistling face formation and multiple contractures to the hands, feet, and face. These symptoms leave patients struggling with tasks such as walking, feeding, breathing, and general self-care. Currently, there are no known therapeutic options for patients with FSS. It has been suggested that FSS mutations result in severe myopathy during embryogenesis, however, the mechanisms by which the mutation disrupts fetal muscle development isn't understood.

Background

FSS

Distal arthrogryposis syndromes are a group of disorders characterized by multiple contractures of the hands, feet, and face. Distal Arthrogryposis Type 2A (DA2A), known as Freeman Sheldon Syndrome (FSS), is the most severe form of Distal arthrogryposis (Bamshad, Ae, & Pleasure, 2009; Freeman & Sheldon, 1938). The cause of FSS has been found to be from mutations in embryonic myosin, MYH3. 90% of FSS cases contain mutations in MYH3, making embryonic myosin the most common cause of distal arthrogryposis syndromes (Beck et al., 2014). FSS presents an ulnar deviation of the wrists and fingers, camptodactyly, microstomia, a whistling face appearance, etc. These symptoms leave patients struggling with basic tasks such as walking, eating, breathing, and mobility (Kulkarni, Panigrahi, Ray, & Marwaha, 2008). Currently, the only therapeutic option for patients with FSS is surgical procedures which are often invasive, risky, and multiple procedures are usually required to fix symptoms such as the whistling face appearance (Ferreira & Minami, 1994; Kalliainen, Drake, Edgerton, Grzeskiewicz, & Morgan, 1983; Stevenson et al., 2006). In addition to surgery, patients are able to go through extensive physical therapy and use assistive devices throughout their daily lives (Sadrimanesh et al., 2013).

Myosin Protein

Myosin is a hexameric protein that has ATPase activity. It consists of a helical coiled-coil, two myosin heads - responsible for catalytic activity, and an essential light chain and regulatory light chain found on both heads (Al-khayat, 2013). The myosin head has ATPase activity, responsible for producing force in the cell. Myosin interacts with a protein called actin in the presence of ATP and undergoes a progression called a power stroke. When ATP is bound to myosin, myosin is not bound to actin and this stage is the “pre-power stroke stage”. The ATP hydrolysis results in a conformational change of the myosin where the head swings back and binds to actin. The myosin performs a “power stroke” which pulls actin against itself, creating movement between the two filaments (Murphy, Rock, & Spudich, 2001).

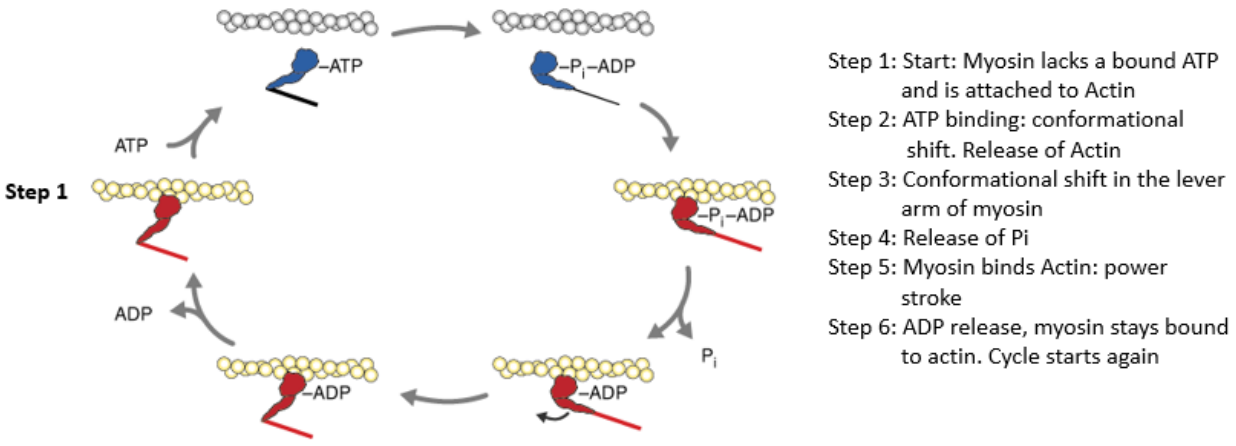

Figure 1: Schematic diagram displaying the Myosin ATPase cycle and associated steps. Actin-bound states are in red, Actin-dissociated states are shown in blue. Image adapted from Murphy, Rock, & Spudich, 2001.

The C-Term of the myosin that forms the helical coiled-coil interacts with other myosins to form the thick filament. The combination of the thick and thin filament, composed of an actin network, form a sarcomere which is the contractile unit of the cell (Al-khayat, 2013). Completion of the ATPase cycle of myosin in the thick filament results in sliding of the thick filament against the thin filament resulting in a contraction. Many sarcomeres undergoing contractions result in muscle movement. This is due to the organization of the sarcomere. Many sarcomeres lined together form a myofibril, multiple myofibrils form muscle fibers (Ferrari, Podugu, & Eskew, 2006). Muscle fibers are the largest entity of muscle that results in muscle movement when multiple sarcomeres contract (Morgan, 1985).

Muscle cells

Three myosin isoforms; embryonic, perinatal, and beta myosin make up the sarcomere composition in muscle cells. Embryonic and perinatal myosin are transiently expressed during embryonic and fetal development, but are downregulated after birth (Schiaffino, Rossi, Smerdu, Leinwand, & Reggiani, 2015). Postnatally, fast and slow myosin become the dominant isoforms after birth (Weiss, Schiaffino, & Leinwand, 1999). The mutation in which FSS is expressed is only found in embryonic myosin, meaning the muscle type where the FSS mutation is found, is primarily expressed up until birth.

The location of mutation T178I is near the nucleotide binding site, suggesting that this mutation may disrupt the ATP binding site (Schiaffino et al., 2015). This could cause a defect in the force produced by myosin. During morphogenesis of the embryo, development is strongly influenced by mechanical forces. Different force production results in a change in the tension of the development of the organism, meaning normal morphogenesis would be altered in cell types, most notably joints and bones could experience abnormal tension and develop differently, if the T178I mutation is disrupting normal force production in the sarcomere (Felsenthal & Zelzer, 2017).

CRISPR

The RNA guided clustered regularly interspaced short palindromic repeats is a revolutionary technique derived from bacteria's immune response to invading DNA phages (Musunuru, 2020; Wyman et al., 2013). The invading material is recognized by an RNA strand that can identify the foreign DNA. Cas9, a protein responsible for the initiating of the immune response, will unwind foreign DNA and check for sequence complimentary to the RNA strand, referred to as the guide RNA. If a match is found, Cas9 will look for a short motif adjacent to the guide RNA called the

protospacer adjacent motif (PAM) sequence. Once located, the Cas9 protein makes a double stranded break. Breaks such as these in the DNA will be repaired by nonhomologous end joining or homology directed repair (Lino et al., 2018). Utilizing homology directed repair, a DNA sequence of interest can be introduced into cells by homology directed repair.

Specific Aims

Question: How does a mutation in embryonic myosin lead to a disease phenotype?

The aim of this work is to investigate the mechanisms in which the FSS causing mutation T178I disrupts development. The data will elucidate early mechanisms by which FSS disrupts development, which will provide insight necessary for subsequent therapeutic intervention of FSS. The aim is broken down into two parts.

Aim 1: What are the functional consequences of the T178I mutation on ATP hydrolysis and muscle contraction?

Aim 2: What are the functional consequences of the T178I mutation in embryonic muscle cells?

Materials and Methods

C2C12 Factories

C2C12 mouse cells are required to produce recombinantly expressed myosin, as these specialized myosins need chaperones to fold. C2C12 cells facilitate the correct folding of myosin. C2C12s are thawed using a 37℃ water bath, cells are resuspended in General Media (GM: DMEM, 20%FBS 1% Pen/Strep 1% L-glut), spun to pellet to remove freeze down media, resuspended in GM and plated on a 10 cm cell culture plate. Cells are split, carried, and expanded until there are enough cells to seed Factories, about 2 15cm plates per factory - 8 factories at a time. Cells are split before they reach 100% confluency, so as to not prematurely differentiate. Once factories are seeded (day 1), cells are grown to 100% confluency as myotubes (day 4). By day 4, media is changed to differentiation media (DM: DMEM, 2% Horse Serum, 1% Pen/Strep 1% L-glut), which changes the C2C12 myoblasts to myotubes. On day 7, the myotubes are infected with a virus. 4 factories are infected with a wildtype (WT) virus to produce embryonic myosin, and 4 factories are infected with a T178I mutant virus to produce embryonic myosin with a T178I mutation. On day 12, cells are lifted from the factories using trypsin, collected, and spun for 30 minutes 3.5K, 4℃. Pellet is frozen in Liquid nitrogen and stored at -80 ℃ until use. Small scale infection experiments showed that this timeline was most efficient for producing myosin protein.

SulfoLink Coupling Resin

Affinity chromatography is used to purify myosin from cell pellets. A column is prepared for affinity chromatography by adding SulfoLink resin (Thermo Fisher) to a column and coupling it with PDZ. The SulfoLink has a free iodoacetyl group that reacts with a sulfhydryl group on the PDZ, creating a conjugated peptide. The column is blocked with L-Cysteine to prevent unwanted binding to free iodoacetyl groups on the SulfoLink resin during purification. The column is stored at 4℃ until use.

Myosin S-1 Ctag Purification from C2C12 Pellets

A cell pellet from the collection of factories is removed from -80℃ and soaked in a Lysis Buffer (100 uL 1 M DTT, 200 uL 0.1 M ATP, ½ PIC). The cell pellet in the buffer is crushed up, or dounced, until it is a homogeneous liquid. The liquid is centrifuged to clarify the pellet, 18K for 25 minutes. The supernatant is collected and filtered, then combined with PDZ linked resin by rocking at 4℃ for 30 minutes to allow binding of the C tag on myosin to the PDZ. The myosin solution is loaded onto a column and allowed to flow through, getting rid of everything in the supernatant, except recombinantly expressed myosin bound to PDZ. The solution is washed (20 mM HEPES, 25 mM KCl, 5 $MgCl_2$, 1mM DTT). An elution buffer is added to the column once the wash drains, buffer 1 with elution peptide and 20 uL DMSO, and incubates with the slurry in the column for 10 minutes. The column is opened and elution fractions from the column are collected. A gel is run using small amounts of each fraction to determine contents within each fraction. Fractions containing recombinantly expressed myosin are combined. Myosin is injected into a cassette and dialyzed in buffer (20 mM HEPES, pH7.5 25 mM KCl 5 mM MgCl2 10% Sucrose 0.5 mM DTT) for 12 hours, then concentrated using PEG for 15 minutes. The concentration of myosin present is determined by a colorimetric assay.

Pierce 660 Assay:

Myosin is taken out of dialysis and stored on ice. BSA in dialysis buffer standards are prepared as a standard curve. Myosin concentration is diluted in half and loaded in triplicate. Pierce 660 buffer (Thermo Fisher) is added to the plate and incubated for 5 minutes. A plate reader determines the absorbance of the solution in this colorimetric assay, and the concentration of myosin is determined from this value by subtracting the absorbance of the blank and dividing that value by the slope of the standard curve. This triplicate value is averaged to determine the concentration of Myosin present from purification.

After completion of the Pierce 660 assay, DTT and ATP are added to myosin and it is flash frozen and kept at -80℃

ATPase Assay

This assay measures the rate of hydrolysis of ATP when myosin undergoes an ATPase cycle when in contact with actin. This is a colorimetric assay. The hydrolysis of ATP is coupled to the

conversion of NADH to NAD+. Since this is a 1 to 1 conversion, the change in absorbance of NADH is directly coupled to the hydrolysis of ATP.

This assay is run by performing a titration of actin onto a plate to get various concentrations of actin. The same amount of myosin is pipetted into each well of varying actin concentrations. ATP, along with NADH, PEP, LDH/PK are added to each well. The plate is measured at 30℃ every 30 seconds for one hour. Analysis is performed by isolating data that encompasses the duration of the reaction cycle, seen as a linear regression. NADH is used as a control. Data is pooled into triplicate and analyzed. A curve is fit to the Michaelis Menten equation, allowing visualization of the amount of actin "turned over" by myosin per second.

Deadhead Spindown

Purified myosin and purified actin are first incubated with ATP, then centrifuged for 25 minutes to pellet the actin. Myosin with an active ATPase domain will release actin and remain in the supernatant, and myosin without an active ATPase domain will be pelleted with the actin. Supernatant and pellet are run out on a gel to determine the proportion of myosin in the supernatant vs pellet. This is done by quantifying off the intensity of the Coomassie stain on the gel. The quantity of deadheads is calculated by %deadhead = (pellet intensity) / (sup+pellet intensity). Myosin in the supernatant is collected and used to perform Motility and ATPase assays.

Motility Assay

Coverslips are coated with nitrocellulose and allowed to dry. A flow cell chamber is constructed using a coverslide, the nitrocellulose treated coverslip, and double-sided sticky tape. Myosin from the deadhead spin is allowed to flow through the cell chamber and given time for the myosin to stick to the nitrocellulose. Any binding sites that weren't taken by myosin are blocked with BSA. Anything left unbound is washed out. Unlabeled actin and ATP are flown through the chamber to bind any deadhead myosin that are bound to the nitrocellulose. TRITC labeled actin and ATP are then flown through the chamber and incubated, then motility buffer is added to the flow cell (Greenberg & Moore, 2011). Visualization of the cell is performed by recording videos under a microscope and analyzing the velocity of the labeled actin. Quantification is performed using MATLAB and the average velocity of the WT and T178I mutant is graphed.

CRISPR

An adenovirus was generated to express the mouse embryonic myosin gene MYH3. The beginnings of making this virus was started but not finished. Two viruses were attempted to be produced, WT and T178I using CRISPR. Each virus includes two plasmids: the first is an expression vector that includes Cas9 and an engineered gRNA, and the second plasmid that acts as the targeting vector for homology directed repair.

The Expression Vector

The expression vector uses plasmid pX330 which includes Cas9 (Joung et al., 2017). Engineered gRNA were chosen to target murine MYH3 exon2. The found gRNA is 23 bp and ends in NGG-3' (PAM sequence). An extra 5' G was added to the gRNA to act as the transcription start for U6 promoter. The final gRNA was inserted into the plasmid, sequencing was performed through a Bbs1 site to confirm insertion.

The Targeting Vector

A synthetic construct was designed and synthetically produced using gene sequence from NCBI on *MYH3*. It includes a left homology arm (LHA), 3' UTR and adjacent downstream sequence, right homology arm (RHA), and restriction sites between. A selection cassette was used from Nautilus4, including 3xpA/pgk PURO r BGHpA. This section was amplified using PCR and inserted into the synthetic construct using recombinant PCR. A wildtype allele including a c-terminal myc epitope was subcloned into pBlueScriptSK+. Recombinant PCR site-directed mutagenesis was performed to introduce the T178I mutation, making a second targeting vector. The two DNA sequences were subcloned into the synthetic construct to produce a WT and T178I targeting vector.

With the completion of the synthesis of the targeting vector and the expression vector, the next step would be to coinfect C_2C_{12} cells to produce CRISPR products. To create the WT cell line, the expression vector and targeting vector without the PCR site-directed mutagenesis would be coinfected. To create the T178I cell line, the expression vector and the targeting vector with the PCR site-directed mutagenesis would be coinfected, creating a cell line with the point mutation.

Results

5.1: *Myosin Purification shows clean fractions for both WT and T178I*

Myosin S-1 Ctag purification from C_2C_{12} cell pellets using affinity chromatography shows clean yields of column 2-5 for both WT and T178I pellets. Cell pellets were collected after being differentiated and infected with virus containing the FSS mutation. Affinity chromatography was performed with PDZ to bind myosin S1 produced by the cells infected with adenovirus. Myosin was eluted off the column and collected into fractions. Gel confirms the fractions that contain virus.

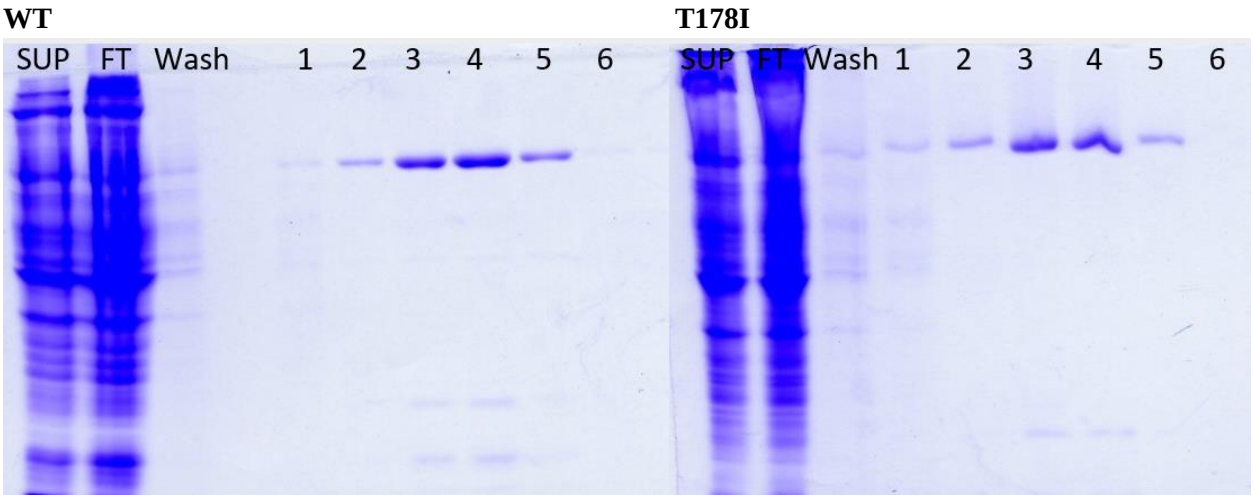

Figure 1: Affinity chromatography of myosin S-1 Ctag using sulfoLink Coupling Resin shows clean yield of wells 2-5 for both WT and T178I fractions.

5.2 *Deadhead spin shows low amounts of deadhead myosin*

A deadhead spin is performed to remove any deadhead myosin from affinity chromatography. After myosin, actin and ATP are spun for 25 minutes, samples are taken from the supernatant and the pellet to check for the ratio of myosin with an active ATPase compared to myosin without an active ATPase, called a deadhead. Densitometry analysis of the bands in ImageJ compares the intensity of Coomassie stained bands to determine proportion of myosin in the supernatant and pellet.

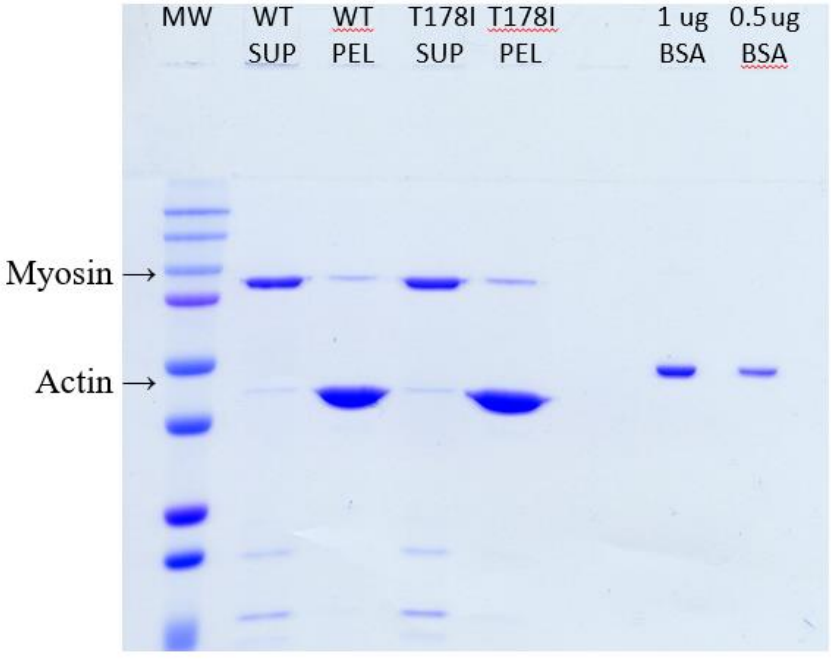

Densitometry Analysis in ImageJ:

WT EmbryonicS1 – **9.6%** deadheads

T178I EmbryonicS1 – **12.3%** deadheads

Figure 2: Analysis of a deadhead spin using a gel to look for the percentage of deadhead myosin compared to active myosin. Gel shows samples from the supernatant and pellet after centrifugation of myosin, actin, and ATP.

5.3 Motility analysis of WT and T178I shows an increased rate of actin movement from the FSS T178I embryonic myosin S1.

A motility assay was performed on the WT and T178I embryonic myosin S1. Video analysis of the fluorescently labeled actin shows that the T178I had a higher velocity than the WT, suggesting that the T178I myosin has a faster turnover rate of actin than the WT.

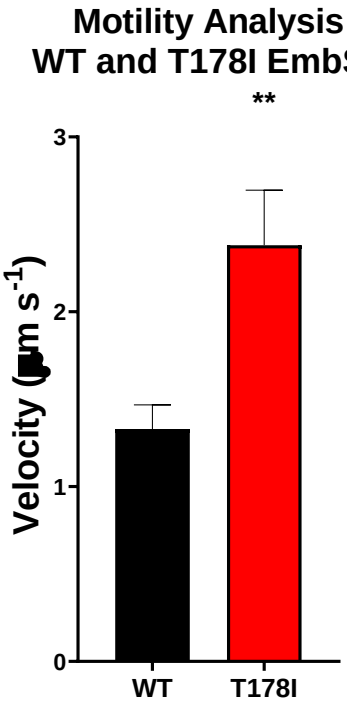

Figure 3: Velocity analysis of the actin filaments shows a significant increase in velocity of the myosin with the FSS causing mutation compared to a wildtype embryonic myosin S1.

5.4: *ATPase analysis shows no change between the T178 mutant myosin and WT myosin*

ATPase analysis, comparing WT myosin to a T178I mutation shows no significant difference in the rate of ATP hydrolysis. The coupled reaction does not have a difference in the level of absorbance measured over an hour. ATPase data was fit to the Michaelis-Menten model of enzyme kinetics to determine k_{cat} and K_M values. k_{cat} is the maximal rate of ATP hydrolysis and K_M is a measurement of the apparent actin affinity. V_0 is the basal ATPase rate with no actin present.

Michaelis-Menten model of kinetics: $V = V_o + \frac{[A] * Kcat}{[A] + Km}$

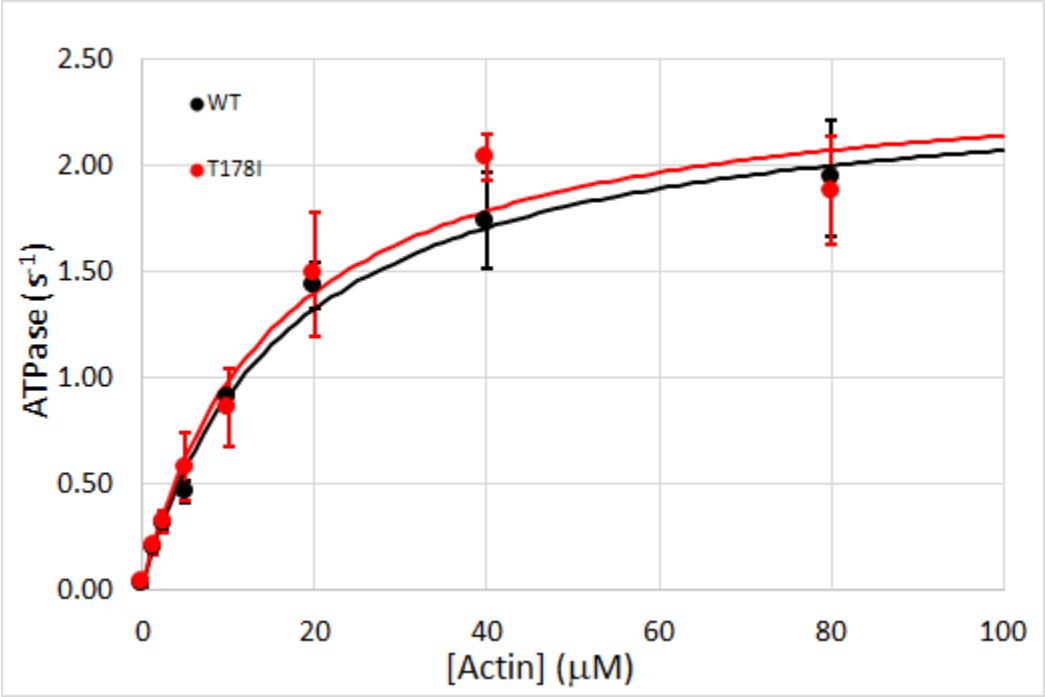

Figure 4: Analysis of WT and T178I embryonic myosin S1 ATPase activity using a coupled reaction to NADH. Absorbance levels are measured and plotted.

ATPase Data Summary Table:

	WT	T178I
k_{cat}	2.38 s-1	2.43 s-1
K_M	16.91 mM	15.56 mM
V_0	0.03	0.04

Table 1: Analysis of the ATPase absorbance levels. The data is fit to the Michaelis Menten equation for enzyme kinetics. Analysis of the maximum rate that the system achieves, and the amount of substrate concentration required to reach half the maximum rate of the system is calculated and reflected in the data table.

5.5 *Gel shows equal myosin loading for the ATPase assay*

After the ATPase assay is complete, a gel controlling for loaded myosin concentrations is run. The gel shows equal loading of myosin present in the sample, confirmed with ImageJ analysis. This data confirms equal myosin concentration for the ATPase assay and analysis.

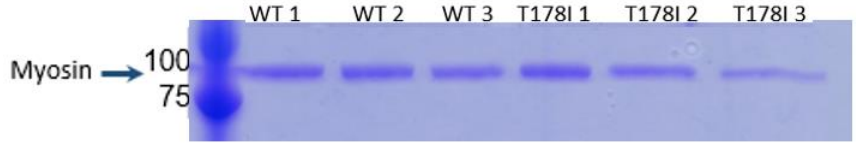

Figure 5: Gel was run to check for equal loading of Embryonic myosin S1 from the ATPase analysis.

Discussion and Future Directions

The ATPase data shows no significant change in the maximal rate of ATP hydrolysis or in actin affinity suggesting that functionally, there is not a biochemical difference of the FSS causing mutation compared to a wild type embryonic myosin.

The motility analysis shows a significant increase in the velocity of T178I mutant compared to the velocity of the WT embryonic myosin. This difference can potentially be explained by two different hypotheses. The first is that either the duty ratio (*f*) or the displacement rate of actin by myosin (*d*). This hypothesis comes from the conclusion that the velocity of the T178I expressing myosin has a significantly higher velocity than the WT. The equation associated with a motility assay is $v = \frac{d*kcat}{f}$. Since there was no significant change in the ATPase data, it can be assumed that the k_{cat} value is not contributing to increase in velocity. To determine if the duty ratio or the step size is a factor, both variables can be studied. Quantifying the step size can be performed by optical trapping and identifying the duty ratio can be studied by performing a second motility assay with varying concentrations of myosin. A curve can be produced by comparing myosin concentration to velocity of the motility assay, and this curve can compare the WT embryonic myosin to the mutant embryonic myosin to determine if there is a change in the duty ratio. The second hypothesis stems from a phenomenon that the SRX/DRX ratio is seen to be altered by myosin mutations. The SRX state characterizes a relaxed and folded back myosin motor. This state renders the myosin unable to interact with actin and the ATPase rate is seen to be at about 10-fold slower than the myosin's basal ATPase rate. The DRX state is also a relaxed state, but the myosin is still able to interact with actin and have active ATPase activity. There has been evidence showing mutations in myosin will shift the SRX/DRX ratio to favor the DRX state, causing more interaction between myosin and actin compared to a myosin without a mutation. This could lead to an increase in velocity of the T178I myosin.

Moving forward with this project, further analysis of the biochemical and motor function of this project to quantify the SRX/DRX ratio of the T178I mutation compared to WT is imperative to determine if this ratio is shifting and altering the mechanical function of the myosin and it's interaction with myosin. Continuing with the CRISPR Cas-9 project may elucidate the mechanisms in which FSS disrupts development by exploring the cellular impact of the T178I mutation. Using the design of the CRISPR-Cas9 constructs, an FSS causing cell line and a WT cell line can be constructed. These cell lines can be analyzed using a Western Blot to look at the abundance of certain muscle proliferation and differentiation markers. Immunostaining of cells can show sarcomere organization and the abundance of developmental markers, which can be used to see if the T178I cell line deviates from the WT differentiation and development into myofibrils. Quantitative Real Time PCR will elucidate development markers at the RNA level.

Beyond cellular work, designing a FSS expressing mouse model may elucidate a correlation between muscle differentiation and bone morphology. Early development is influenced by morphological cues such as stiffness and tension, so if myosin acts in an abnormal fashion during development, this may track with the phenotype associated with FSS.

Limitations: It is important to acknowledge that the work for this project has been performed in mouse cells and with myosin from recombinantly expressed mouse myosin. Therefore, the translation between mouse to human regarding the FSS mutation T178I may not be transparent.

This choice was made due to the limitations with using human samples. There are only a handful of patients that contain the FSS mutation, so acquiring human samples is near impossible. Differentiating human iPSC to skeletal muscle is in the preliminary stages and is only limitedly available for usage, therefore using mouse cells was the best approach for this project to study FSS. However, considerations should be made to move this project into a human cell line if possible.

Conclusion

The aim of this data was to understand how a mutation in embryonic myosin could lead to a disease phenotype. Freeman Sheldon Syndrome is expressed in embryonic myosin, which is downregulated after birth, yet a phenotype persists into adulthood. This data characterizes the FSS causing T178I mutation which is the most severe mutation to date. Biochemical and mechanical analysis is performed by a motility assay and ATPase assays. Analysis of the functional consequences of T178I in cells is proposed in this project by designing a cloning strategy using CRISPR-Cas9 to produce a T178I cell line.

The data shows that there is no biochemical difference between the T178I cell line compared to the WT cell line, however a mechanical difference was detected in the motility analysis. This discrepancy can be explained by a difference in the duty ratio and the displacement rate of actin by myosin or by a change in the SRX/DRX ratio. Future studies can focus on identifying the SRX/DRX ratio and the duty ratio of myosin. Production and characterization of a T178I cell line can be studied to elucidate potential disruptions in development.

Acknowledgments

This work was supported by Beckman Scholars Program, Biological Sciences Initiative, and the University of Colorado Boulder Undergraduate Research Opportunities Program.

I would like to thank Dr. Leslie Leinwand for the mentorship and the opportunity to pursue undergraduate research. It has been an honor and a privilege working in the Leinwand Lab for the last 4 years, and my college career has been greatly enhanced from this experience. Dr. Leinwand has taught me what successful scientific research looks like and the importance of using the work of my predecessors to constantly improve on the knowledge of the field.

Thank you to Dr. Kristi Anseth for her expertise and insightfulness in helping form and perfect my thesis.

Thank you to Dr. Pamela Harvey for advising my thesis and allowing me to play a role as a mentor to other students, further broadening my experience in the field of academia.

I would like to thank Dr. Maureen Bjerke, Dr. Anastasia Karabina, Dr. Stephen Langer, Dr. Sarah Lehman, and Dr. Kristen Bjorkman for their support during my time as an undergraduate. Dr. Kristen Bjorkman instilled a love for Biology and encouragement to pursue research, all of which set me on the path that I am on today. Dr. Anastasia Karabina, Dr. Maureen Bjerke, Dr. Sarah Lehman and Dr. Stephen Langer have invested countless hours at the bench teaching me methods and advising my project. Without them, I'd be lost.

Finally, I would like to thank my parents, my family, and my friends for their support in the completion of my degree and thesis.

References

Al-khayat, H. A. (2013). Review article Three-dimensional structure of the human myosin thick filament : clinical implications.

Bamshad, M., Ae, H., & Pleasure, D. (2009). Arthrogryposis: A Review and Update, 40–46. https://doi.org/10.2106/JBJS.I.00281

Beck, A. E., Mcmillin, M. J., Gildersleeve, H. I. S., Shively, K. M. B., Tang, A., Bamshad, M. J., & Al, B. E. T. (2014). Genotype-Phenotype Relationships in Freeman – Sheldon Syndrome, (September), 2808–2813. https://doi.org/10.1002/ajmg.a.36762

Felsenthal, N., & Zelzer, E. (2020). Mechanical regulation of musculoskeletal system development, *144*(23), 4271–4283. https://doi.org/10.1242/dev.151266

Ferrari, M. B., Podugu, S., & Eskew, J. D. (2006). Assembling the Myofibril, *45*(28), 317–337.
Ferreira, L. M., & Minami, E. (1994). Case Report Freeman-Sheldon syndrome : surgical correction of microstomia, 1–2.
Freeman, J. H., & Sheldon, E. A. (1938). CRANIO-CARPO-TARSAL DYSTROPHY, *1937*, 277–283.
Greenberg, M. J., & Moore, J. R. (2011). The Molecular Basis of Frictional Loads in the In Vitro Motility Assay with Applications to the Study of the Loaded Mechanochemistry of Molecular Motors, *67*(5), 273–285. https://doi.org/10.1002/cm.20441.The
Joung, J., Konermann, S., Gootenberg, J. S., Abudayyeh, O. O., Platt, R. J., Brigham, M. D., … Zhang, F. (2017). Genome-scale CRISPR-Cas9 knockout and transcriptional activation screening. *Nature Protocols*, 31–33. https://doi.org/10.1038/nprot.2017.016
Kalliainen, L. K., Drake, D. B., Edgerton, M. T., Grzeskiewicz, J. L., & Morgan, R. F. (1983). Surgical Management of the Hand in Freeman-Sheldon Syndrome, (patient 2).
Kulkarni, K. P., Panigrahi, I., Ray, M., & Marwaha, R. K. (2008). Distal arthrogryposis syndrome, *14*(2), 67–69. https://doi.org/10.4103/0971-6866.44108
Lino, C. A., Harper, J. C., Carney, J. P., Timlin, J. A., Lino, C. A., Harper, J. C., … Timlin, J. A. (2018). Delivering CRISPR : a review of the challenges and approaches Delivering CRISPR : a review of the challenges and approaches. *Drug Delivery*, *25*(1), 1234–1257. https://doi.org/10.1080/10717544.2018.1474964
Morgan, B. Y. D. L. (1985). FROM SARCOMERES TO WHOLE MUSCLES, *78*, 69–78.
Murphy, C. T., Rock, R. S., & Spudich, J. A. (2001). A myosin II mutation uncouples ATPase activity from motility and shortens step size, *3*(March), 311–315.
Musunuru, K. (2020). The Hope and Hype of CRISPR-Cas9 Genome Editing. *JAMA Cardiol. 2017;2(8):914–919.* https://doi.org/10.1001/jamacardio.2017.1713
Sadrimanesh, R., Hassani, A., Aliakbar, S., Chaghari, H., Sadr-eshkevari, P., & Rashad, A. (2013). Freeman e Sheldon syndrome : Combined surgical and non-surgical approach. *Journal of Cranio-Maxillofacial Surgery*, *41*(5), 397–402. https://doi.org/10.1016/j.jcms.2012.11.004
Schiaffino, S., Rossi, A. C., Smerdu, V., Leinwand, L. A., & Reggiani, C. (2015). Developmental myosins : expression patterns and functional significance. *Skeletal Muscle*, 1–14. https://doi.org/10.1186/s13395-015-0046-6
Stevenson, D. A., Carey, J. C., Palumbos, J., Rutherford, A., Dolcourt, J., & Bamshad, M. J. (2006). Clinical Characteristics and Natural History of Freeman-Sheldon Syndrome. *Pediatrics*, *117*(3), 754 LP-762. https://doi.org/10.1542/peds.2005-1219
Weiss, A., Schiaffino, S., & Leinwand, L. A. (1999). Comparative Sequence Analysis of the Complete Human Sarcomeric Myosin Heavy Chain Family : Implications for Functional Diversity.
Wyman, J., Changeux, J. P., Filmer, D., Jovin, T. M., Baehr, W., Holbrook, J. J., … Bustamante, C. (2013). Multiplex Genome Engineering Using CRISPR/Cas Systems, (February), 819–824.